Journal of Oleo Science
Copyright ©2013 by Japan Oil Chemists' Society
J. Oleo Sci. **62**, (12) 1017-1027 (2013)

Interfacial Properties in Langmuir Monolayers and LB Films of DPPC with Partially Fluorinated Alcohol (*F8H7*OH)

Hiromichi Nakahara, Chikayo Hirano, Ichiro Fujita and Osamu Shibata*

Department of Biophysical Chemistry, Faculty of Pharmaceutical Sciences, Nagasaki International University; 2825-7 Huis Ten Bosch, Sasebo, Nagasaki 859-3298, Japan

Abstract: Two-component interactions between (perfluorooctyl) heptanol (*F8H7*OH) and dipalmitoylphosphatidylcholine (DPPC), which is a major component of pulmonary surfactants in mammals, were systematically elucidated using Langmuir monolayers and Langmuir-Blodgett (LB) films of the compounds. The interactions such as the miscibility of the compounds and their phase behavior were examined from thermodynamic and morphological perspectives. The surface pressure (π)–molecular area (A) and surface potential (ΔV)–A isotherms of the binary monolayers containing *F8H7*OH in different mole fractions (X_{F8H7OH}) were measured simultaneously. The excess Gibbs free energy of mixing of the two components was calculated from the π–A isotherms. The resulting isotherm data were employed to construct a two-dimensional (2D) phase diagram of the system. The phase diagram revealed that the transition pressure as well as the monolayer collapse pressure change with changes in X_{F8H7OH}. These thermodynamic analyses suggested that the miscibility of the two components and the solidification of DPPC monolayers can be induced by the addition of *F8H7*OH. The phase behavior upon monolayer compression was observed morphologically *in situ* using Brewster angle microscopy (BAM) and fluorescence microscopy (FM), as well as *ex situ* using atomic force microscopy (AFM). Interestingly, the AFM-based analysis revealed the formation of monodispersed 2D micelles consisting of *F8H7*OH at low surface pressures.

Key words: Langmuir monolayer, pulmonary surfactant, DPPC, fluorinated amphiphile, surface pressure, surface potential

1 INTRODUCTION

Fluorinated amphiphiles have attracted great interest, largely owing to their unique properties, including their hydrophobicity and lipophobicity[1], high gas-dissolving capacity, chemical and biological inertness, low surface tension, and high fluidity[1, 2]. Partially fluorinated compounds often form monodisperse two-dimensional (2D) micelles at the air-water interface. This is a characteristic property associated with monolayers, and these micelles can be observed using atomic force microscopy (AFM)[3–5]. The potential applications of these compounds in medicine, particularly in disease diagnosis and therapy, have made them the target of numerous investigations[1, 6, 7]. Further, while it has been shown that fluorinated compounds tend to accumulate in the environment and in the human body[8–11], this is not always the case. For example, perfluorooctyl bromide (PFOB) has been shown to have short organ retention times and can potentially be used for oxygen delivery[12, 13]. Thus, compounds that have been fluorinated to a low degree should have high or at least partial applicability in numerous industrial fields and areas of medicine.

Dipalmitoylphosphatidylcholine (DPPC) is a major component of native pulmonary surfactants (PS)[14–16]. PS films at the air-alveolar fluid interface undergo successive changes in fluidity and rigidity during compression and expansion. DPPC contributes significantly to the rigidity of these PS films. However, such films can exhibit slow adsorption and poor diffusion at their surfaces. Herein, we describe the effects of fluorinated compounds on the fluidity, phase behavior, and interfacial properties of DPPC monolayers. The effects that perfluorocarboxylic acids[17, 18] and partially fluorinated amphiphiles[19–23] have on DPPC monolayers have been investigated previously. Recently, partially fluorinated alcohols of $CF_3(CF_2)_7(CH_2)_mOH$ ($m=5$

*Correspondence to: Osamu Shibata, Department of Biophysical Chemistry, Faculty of Pharmaceutical Sciences, Nagasaki International University, 2825-7 Huis Ten Bosch, Sasebo, Nagasaki 859-3298, Japan
E-mail: wosamu@niu.ac.jp
Accepted July 1, 2013 (received for review April 27, 2013)
Journal of Oleo Science ISSN 1345-8957 print / ISSN 1347-3352 online
http://www.jstage.jst.go.jp/browse/jos/ http://mc.manusriptcentral.com/jjocs

(or *F*8*H*5OH) and 11 (or *F*8*H*11OH)) have been shown to improve PS functionality, allowing for greater control over monolayer fluidity and hysteresis behavior[24].

In the present study, we employed Langmuir monolayers to investigate the interfacial behavior and lateral interactions of binary systems containing the fluorinated alcohol $CF_3(CF_2)_7(CH_2)_7OH$ (or *F*8*H*7OH) and DPPC. This was done using surface pressure (π)–molecular area (A) and surface potential (ΔV)–A isotherms, Brewster angle microscopy (BAM), fluorescence microscopy (FM), and AFM. *F*8*H*7OH was compared with *F*4*H*11OH, which has the same hydrophobic chain length of 15 carbons as *F*8*H*7OH. The binary miscibility of DPPC and *F*4*H*11OH has already been characterized previously[19]. The excess Gibbs free energy of mixing and the interaction parameter (or energy) of the binary system were obtained from the π–A isotherm data. The miscibility of the two components was also elucidated from both thermodynamic and morphological perspectives.

2 EXPERIMENTAL

2.1 Materials

(Perfluorooctyl)heptanol (*F*8*H*7OH) was synthesized using a known protocol[25]. L-α-Dipalmitoylphosphatidylcholine (DPPC; purity > 99%) and the fluorescent probe 1-palmitoyl-2-[6-[(7-nitro-2-1,3-benzoxadiazol-4-yl)amino]hexanoyl]-*sn*-glycero-3-phosphocholine (NBD-PC) were obtained from Avanti Polar Lipids (Alabaster, AL, USA) and were used without further purification. *n*-Hexane (>98.5%) and ethanol (>99.5%) were obtained from Merck KGaA (Uvasol, Darmstadt, Germany) and nacalai tesque (Kyoto, Japan), respectively. An *n*-hexane/ethanol (9/1, v/v) mixed solvent system was used for spreading the binary system. Sodium chloride (nacalai tesque) was roasted at 1023 K for 24 h to remove all surface-active organic impurities. The subphase solution was prepared using thrice-distilled water (surface tension = 72.0 mN m^{-1} at 298.2 K; electrical resistivity = 18 MΩ cm).

2.2 Methods

2.2.1 Surface pressure–area isotherms

The surface pressures (π) of the monolayers were measured using an automated, custom-made Wilhelmy balance. The surface pressure balance used (AG-245, Mettler Toledo) had a resolution of 0.01 mN m^{-1} and was equipped with filter paper (Whatman 541, periphery = 4 cm). The trough was made from Teflon-coated brass (area = 720 cm^2). Both hydrophobic and lipophobic Teflon barriers were used in this study. The π–molecular area (A) isotherms were recorded at 298.2 ± 0.1 K. Stock solutions of DPPC (1.0 mM) and *F*8*H*7OH (1.0 mM) were prepared in *n*-hexane/ethanol (9/1, v/v). The spreading solution was allowed to evaporate for 15 min prior to the compression of the monolayers. The monolayers were compressed at a rate of ~0.10 nm^2 molecule^{-1} min^{-1}. The standard deviations (SD) for A and π were ~0.01 nm^2 and ~0.1 mN m^{-1}, respectively[21, 26, 27].

2.2.2 Surface potential–area isotherms

The surface potential (ΔV) and π values were recorded simultaneously when the monolayers were compressed at the air-water interface. The process was monitored using an ionizing ^{241}Am electrode positioned 1–2 mm above the interface, while a reference electrode was dipped into the subphase. A Keithley 614 electrometer was used for the ΔV measurements. The SD for ΔV was 5 mV[28, 29].

2.2.3 Brewster angle microscopy (BAM)

The monolayers were imaged directly at the air-water interface using a Brewster angle microscope (KSV Optrel BAM 300, KSV Instruments Ltd., Finland) coupled to a film balance system (KSV Minitrough, KSV Instruments Ltd.). Using a 20 mW He–Ne laser, which emitting *p*-polarized light with a wavelength of 632.8 nm, and a 10× objective lens in combination allowed for a lateral resolution of ~2 μm. The angle of the incident beam to the interface was fixed to the Brewster angle (53.1°) at 298.2 K. The reflected beam was recorded with a high-grade charge-coupled device (CCD) camera (EHDkamPro02, EHD Imaging GmbH, Germany)[20, 21, 30].

2.2.4 Fluorescence microscopy (FM)

The film balance system (KSV Minitrough) was mounted on the stage of an Olympus microscope BX51WI (Tokyo, Japan) that was equipped with a 100 W mercury lamp (USH-1030L), an objective lens (SLMPlan; 50×, working distance = 15 mm) and a 3CCD camera with a camera control unit (IKTU51CU, Toshiba, Japan). The spreading solution of the cosolubilized samples was prepared as described earlier and was then doped with 1 mol% of the fluorescence probe (NBD-PC). Image processing and analysis were performed using Adobe Photoshop Elements ver. 7.0 (Adobe Systems Inc., CA). The total amount of ordered domains (dark-contrast regions or those not containing NBD-PC) was determined and expressed as a percentage per frame by dividing the respective frame into dark and bright regions. The resolution was 0.1%, and the maximum SD was 8.9%. The procedure for the FM-based measurements is mentioned in detail in previous reports[20, 24].

2.2.5 Atomic force microscopy (AFM)

Langmuir-Blodgett (LB) films were prepared using the KSV Minitrough. Freshly cleaved mica (Okenshoji Co., Tokyo, Japan) was used as a supporting solid substrate for film deposition, which was performed through the vertical dipping method. The transfer velocity during the single-layer deposition process, which was performed at selected surface pressures, was 5 mm min^{-1}. The film-forming materials were spread on 0.15 M NaCl at 298.2 K. During the transfer process, the hydrophilic part of the monolayer is

in contact with the mica substrate while the hydrophobic part is exposed to air. LB films deposited at a rate of ~1 were used in the subsequent experiments. All AFM-based observations were made in air at room temperature. The images were obtained using an SPA 400 instrument (Seiko Instruments Co., Chiba, Japan) in the tapping mode. This provided both topographical and phase-contrast images. The procedure for performing the AFM-based analysis has been reported in detail elsewhere[19, 26].

3 RESULTS AND DISCUSSION

3.1 π–A and ΔV–A isotherms

A thermal analysis of *F8H7*OH in the solid state has been reported[25]. Its melting point was determined to be 338.8 K, which is approximately 22 K higher than that of the corresponding hydrogenated alcohol (pentadecanol)[31]. A 2D monolayer of *F8H7*OH is stable on water at temperatures lower than 298.2 K; this result is consistent with the properties typically associated with ordered monolayers and an increase in the surface pressure (π)[25].

The π–A and ΔV–A isotherms of the binary DPPC/*F8H7*OH system obtained on 0.15 M NaCl at 298.2 K are shown in Fig. 1. It is known that DPPC monolayers (*Curve 1*) undergo a liquid-expanded (LE)/liquid-condensed (LC) phase transition at ~11 mN m^{-1} (dashed arrow)[22, 23, 26, 32]. In contrast to DPPC, *F8H7*OH forms a typical ordered monolayer (*Curve 7*), which collapses at ~54 mN m^{-1} (A = 0.23 nm^2). Upon the monolayer's collapse, its conversion from a 2D monolayer to the three-dimensional (3D) bulk state can be observed at the air-water surface. The limiting area of *F8H7*OH monolayers is ~0.33 nm^2 and is similar to the cross-sectional area of the *F*-chains (~0.30 nm^2)[1]. The π–A isotherms for the two components shift to smaller areas (*Curves 2–6*) as the mole fraction of *F8H7*OH (X_{F8H7OH}) is increased. The transition pressure, π^{eq}, that is, the pressure at which the monolayer phases begin to shift from disordered to ordered states remains largely unchanged when $0 \le X_{F8H7OH} \le 0.3$ but decreases when $X_{F8H7OH} > 0.3$. As such, at low surface pressures, the DPPC and *F8H7*OH monolayers are miscible for $0 \le X_{F8H7OH} \le 0.3$ and solidify for $X_{F8H7OH} > 0.3$[18, 20]. Furthermore, the collapse pressure, π^c, apparently changes with X_{F8H7OH}, implying that the two components are miscible in the monolayer state.

The ΔV–A isotherms show that the DPPC (*Curve 1*) and *F8H7*OH (*Curve 7*) monolayers exhibit contrasting behavior. A positive variation was observed in the case of the DPPC monolayer with respect to A, while a negative variation was seen in the case of the *F8H7*OH monolayer. The nature of ΔV (positive or negative) upon monolayer compression has been studied previously[18, 20, 21]. The magnitude of ΔV increases upon lateral compression as the hydrophobic moieties of the monolayer-forming amphiphilic molecules are oriented towards air and the hydrophilic groups are positioned within the subphase. The ΔV–A isotherms of the DPPC monolayers exhibit a sharp jump (~320 mV) in the vicinity of the onset of the corresponding π–A isotherm, that is, at the point where the π values begin to increase from zero. This jump corresponds to the transition from the gaseous phase to the LE phase. For $0 \le X_{F8H7OH} \le 0.5$, the magnitude of the jump decreases and becomes unclear in terms of appearance and value with increases in X_{F8H7OH}. The ΔV–A isotherms for the system shift from positive to negative values as X_{F8H7OH} increases; this result is consistent with the behavior of other hydrocarbon–fluorocarbon systems[18, 21, 27].

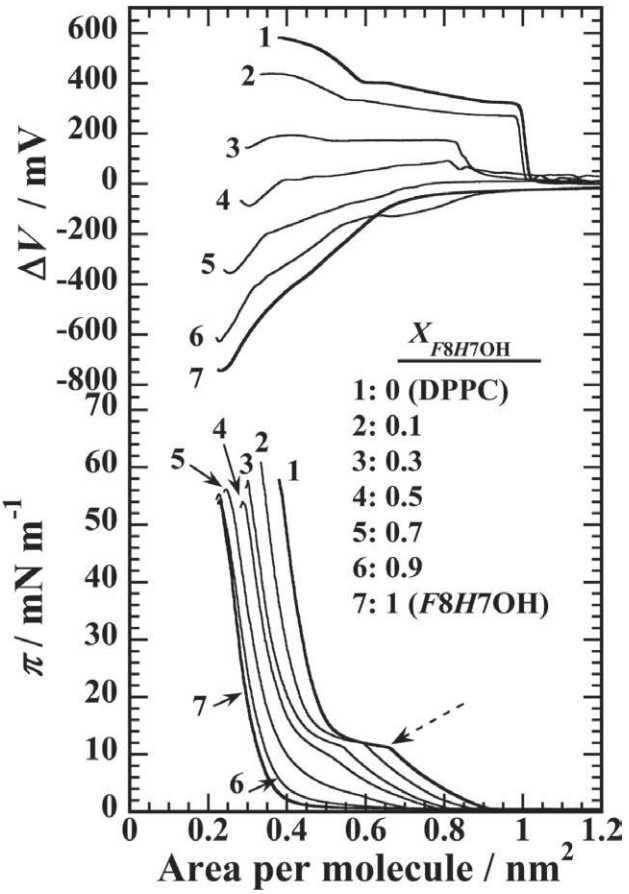

Fig. 1 The π–A and ΔV–A isotherms of the binary DPPC/*F8H7*OH monolayers on 0.15 M NaCl at 298.2 K.

3.2 Excess Gibbs free energy

The interactions between DPPC and *F8H7*OH within a monolayer can be analyzed in terms of the excess Gibbs free energy of mixing (ΔG_{mix}^{exc}) of the compounds, which can be calculated using the following equation (Eq. (1))[33]:

$$\Delta G_{mix}^{exc} = \int_0^{\pi} (A_{12} - X_1 A_1 - X_2 A_2)\, d\pi \qquad (1)$$

where A_i and X_i are the molecular area and mole fraction

of component i, respectively, and A_{12} is the mean molecular area of the binary monolayer. For identical interactions between the two components, ΔG^{exc}_{mix} is zero. This indicates that they are either ideally mixed in the monolayer or are not mixed completely, resulting in patched-like packing[34, 35]. A negative ΔG^{exc}_{mix} value indicates that an attractive interaction exists between the two components. The ΔG^{exc}_{mix}–X_{F8H7OH} plot for DPPC/*F*8*H*7OH at representative surface pressures is shown in Fig. 2. At $X_{F8H7OH} = 0.9$, that is, when the monolayer is in an ordered state for whole surface pressures greater than 1 mN m^{-1} (Fig. 1), the ΔG^{exc}_{mix} value decreases with an increase in the surface pressure. For $0 < X_{F8H7OH} \leq 0.7$, however, the monolayers exhibit complicated behavior with respect to the surface pressure. This is attributed to the different phases of the monolayers (disordered and ordered), which are caused by the changes in π^{eq} by the variations in X_{F8H7OH}. For example, the monolayers corresponding to $0 < X_{F8H7OH} < 0.7$ exhibited disordered phases, while that corresponding to $X_{F8H7OH} = 0.7$ exhibited an ordered phase at 5 mN m^{-1}. Thus, taking these types of defects into account, it was found that the results of the ΔG^{exc}_{mix} analysis for pressures greater than 25 mN m^{-1} provide a better understanding of the mutual interactions between the components because the monolayers are in the ordered phase irrespective of the surface pressure. The ΔG^{exc}_{mix} values for the entire range of X_{F8H7OH} values except for $X_{F8H7OH} = 0.2$ ranged from 200 to −200 J mol^{-1}. These values are quite small in terms of the interaction between the two components. At $X_{F8H7OH} = 0.2$, however, significant changes were noticed in ΔG^{exc}_{mix}. As the surface pressure increases, its value reaches the minimum (∼ −800 J mol^{-1}) at 45 mN m^{-1}. This behavior suggests that the attractive force between the hydrophobic chains of DPPC and *F*8*H*7OH increases upon compression and that the affinity between the two components is the highest at $X_{F8H7OH} = 0.2$. Therefore, these results provide further evidence of two-component miscibility within a monolayer.

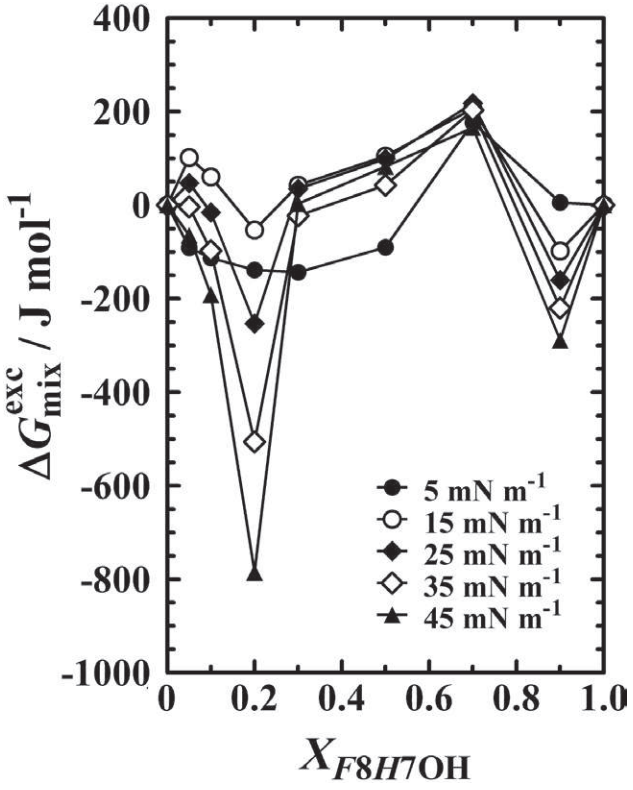

Fig. 2 Excess Gibbs free energy of mixing (ΔG^{exc}_{mix}) of the binary DPPC/*F*8*H*7OH monolayers as a function of X_{F8H7OH} at typical surface pressures on 0.15 M NaCl at 298.2 K.

3.3 Two-dimensional phase diagrams

Shown in Fig. 3 is a 2D phase diagram for the binary system at 298.2 K; the diagram was constructed by plotting the π^{eq} and π^{c} values against X_{F8H7OH}. The π^{eq} values remain almost constant for $X_{F8H7OH} \leq 0.3$. However, π^{eq} decreases as X_{F8H7OH} increases from 0.3 to 0.7. The experimentally determined π^{c} values also varied with X_{F8H7OH}. Accordingly, the two components could be said to be miscible in the monolayer state. The coexistence phase boundary between the monolayer phase (2D) and the bulk phase (3D) of the molecules spread on the surface can be theoretically simulated using the Joos equation[36, 37] and assuming a regular surface mixture:

$$1 = x_1^s \exp\{(\pi_m^c - \pi_1^c)\omega_1 / kT\} \exp\{\xi (x_2^s)^2\} + x_2^s \exp\{(\pi_m^c - \pi_2^c)\omega_2 / kT\} \exp\{\xi (x_1^s)^2\} \quad (2)$$

where x_1^s and x_2^s represent the mole fractions of components 1 and 2, respectively, in the two-component monolayer; π_1^c and π_2^c are the collapse pressures of components 1 and 2, respectively; π_m^c is the collapse pressure of the binary monolayer at a given value of x_1^s (or x_2^s); ω_1 and ω_2 are the molecular areas of components 1 and 2, respectively, at the monolayer collapse pressure; ξ is the interaction parameter; and kT is the product of the Boltzmann constant and the temperature in Kelvin. A solid curve could be obtained at higher surface pressures by adjusting the interaction parameter in Eq. (2) so as to achieve the best fit for the experimentally determined π^{c} values. It is should be noted that the binary system exhibited both negative and positive interaction parameters as well as different interaction behavior in the two regions: $\xi = -3.03$ for $0 \leq X_{F8H7OH} \leq 0.3$ and $\xi = 0.67$ for $0.3 \leq X_{F8H7OH} \leq 1$.

The interaction energy ($\Delta\varepsilon$) is given as follows:

$$\Delta\varepsilon = \xi RT/z \quad (3)$$

where z is the number of nearest neighbors per molecule (equal to 6 in this case) in a closely packed monolayer. The expression for the interaction energy can be rewritten as $\Delta\varepsilon = \varepsilon_{12} - (\varepsilon_{11} + \varepsilon_{22})/2$[36], where ε_{12} denotes the potential

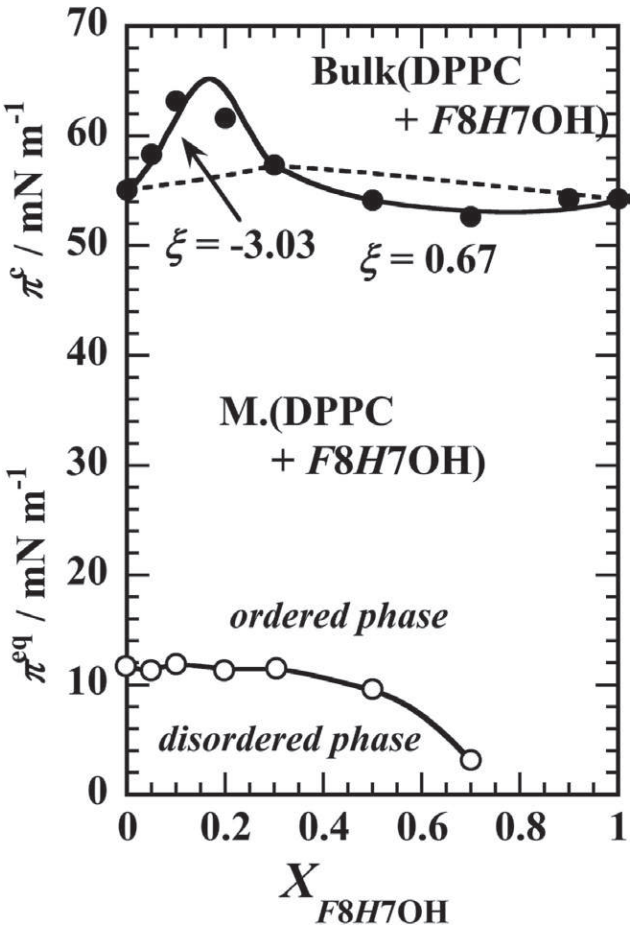

Fig. 3 Two-dimensional phase diagrams based on the variation of the transition pressure (π^{eq}: open circle) and collapse pressure (π^{c}: solid circle) on 0.15 M NaCl at 298.2 K as a function of X_{F8H7OH}. The dashed lines were calculated according to Eq. (2) for $\xi = 0$. The solid line at high surface pressures was obtained by curve fitting of experimental π^{c} to Eq. (2). **M**. indicates a mixed monolayer formed by DPPC and *F*8*H*7OH species, whereas **Bulk** denotes a solid phase of DPPC and *F*8*H*7OH (''bulk phase" may be called "solid phase").

interaction energy between components 1 and 2. The calculated interaction energies were -1267 J mol^{-1} ($\xi = -3.03$) and 277 J mol^{-1} ($\xi = 0.67$). That is to say, the DPPC–*F*8*H*7OH interaction was found to be stronger than similar DPPC–DPPC and *F*8*H*7OH–*F*8*H*7OH interactions for $0 \le X_{F8H7OH} \le 0.3$. On the other hand, the DPPC–*F*8*H*7OH interaction becomes weaker for the other range of X_{F8H7OH} values. Nevertheless, the two components were miscible within a monolayer, since the interaction energies of the two components were smaller than $2RT$ (4959 J mol^{-1}).

For $0 \le X_{F8H7OH} \le 0.3$, the two components did not interact favorably at low surface pressures. This was because the values of π^{eq} remained almost constant with respect to X_{F8H7OH}. However, the large negative ξ value at high surface pressures was indicative of the strong interaction between them. On the other hand, the phase diagram for $0.3 \le X_{F8H7OH} \le 1$ exhibits behavior that is the opposite of that seen in the case of $0 \le X_{F8H7OH} \le 0.3$. This is not the case generally when the interaction mode remains the same over the whole surface pressures. To the best of our knowledge, monolayers of the binary DPPC/*F*4*H*11OH system are similar to those of the DPPC/*F*8*H*7OH system[19]. However, the fluidization of the DPPC monolayers occurs in the case of the DPPC/*F*4*H*11OH system, whereas the monolayers are solidified by the addition of *F*8*H*7OH. The interaction parameter for the DPPC/*F*8*H*7OH system ($\xi = -3.03$) is almost the same as that for the DPPC/*F*8*H*11OH system ($\xi = -3.13$)[20] in the DPPC-rich region but is considerably larger than that for the DPPC/*F*4*H*11OH system ($\xi = -1.57$)[19]. That the parameter values for *F*8*Hm*OH systems are larger can be attributed to the fact that the cohesive force between the perflurooctylated hydrocarbon (*F*8*Hm*OH) and hydrocarbon (DPPC) chains is greater. This is because the fluorinated chain in the *F*4*H*11OH molecules is shorter by four perfluorinated methylene groups.

3.4 BAM observations

In situ morphological observations of the binary DPPC/*F*8*H*7OH monolayers were performed using BAM in order to elucidate their phase behaviors. BAM images of the monolayers corresponding to $X_{F8H7OH} = 0$ (DPPC), 0.05, 0.1, and 0.2 are shown in Fig. 4. All of the BAM images exhibit coexisting disordered (dark contrast) and ordered (bright contrast) phases. The images of the DPPC monolayers were homogeneously dark for π^{eq} values lower than $\sim$11 mN m^{-1} (data not shown). In the case of monolayer compression at pressures greater than $\sim$11 mN m^{-1}, LC domains are formed, and these increase in size and number, as can be seen from Fig. 4 (column 1). Finally, the image becomes optically bright for pressures greater than 25 mN m^{-1} [20,24]. The images of the *F*8*H*7OH monolayers remained homogeneous in contrast irrespective of the surface pressure (data not shown). It is widely accepted that domain formation is controlled by a balance between the line tension at the boundary between the disordered and ordered domains and the long-range dipole-dipole interactions between the ordered domains. Therefore, it was found that the dipole-dipole interactions were stronger in the LC domains of the DPPC monolayers[38]. In the case of the monolayers corresponding to $X_{F8H7OH} = 0.05$, the effect of *F*8*H*7OH on the LC domains of the DPPC monolayers was insignificant. However, the addition of *F*8*H*7OH in greater amounts changed the shape of the domain, making it round; this was true for $X_{F8H7OH} = 0.1$ and 0.2. The domain also grows in size as the surface pressure is increased. This means that

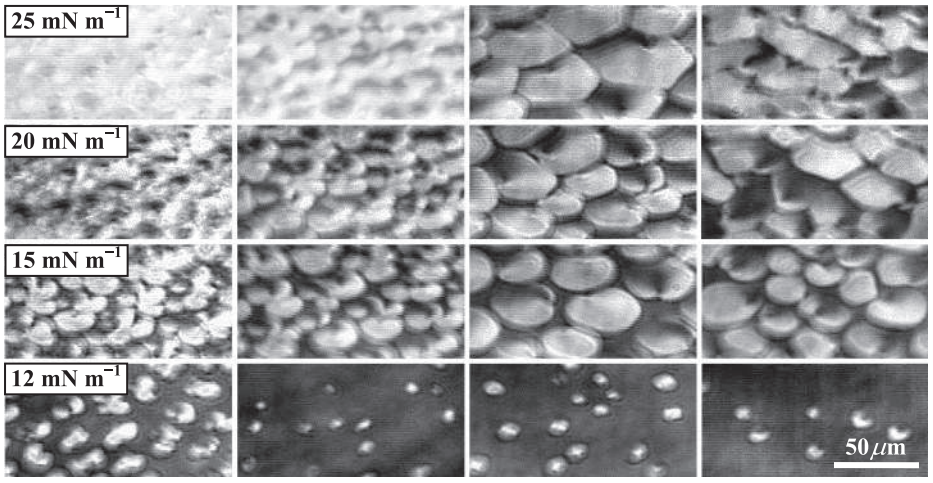

Fig. 4 BAM images of the binary DPPC/*F*8*H*7OH monolayers for $X_{F8H7OH} = 0$ (DPPC), 0.05, 0.1, and 0.2 at 12, 15, 20, and 25 mN m^{-1} on 0.15 M NaCl at 298.2 K. The scale bar in the lower right represents 50 μm.

the effect of the line tension on domain formation becomes more significant. In this case, the addition of *F*8*H*7OH in an amount corresponding to $X_{F8H7OH} = 0.3$ produces homogeneous dark images for all the whole surface pressures (data not shown). At 12 mN m^{-1}, the ratio of the ordered domains is somewhat low compared to that of the DPPC. This is attributed to the fact that the mutual interaction between the two components is relatively weak owing to the large intermolecular distance, which is the result of the weak van der Waals attraction between the fluorocarbon molecules. Furthermore, the corresponding FM images (Fig. 5) provided further evidence of the phenomenon. The results of the observations for $X_{F8H7OH} \geq 0.3$ are discussed in detail in the next section.

3.5 FM observations

Shown in Fig. 5 are the *in situ* micrographs of the DPPC/*F*8*H*7OH monolayers obtained using FM. In the FM images, the bright and dark contrasts correspond to the disordered and ordered phases, respectively, as opposed to the corresponding BAM images (Fig. 4). FM allows for morphological images of higher resolution, magnification, and contrast compared to those achievable using BAM. The FM images of the DPPC monolayers (the first column) indicated the coexistence of the LE and LC phases. The shape of the LC domain is characteristic of DPPC monolayers and has been discussed previously[20, 21, 39, 40]. At $X_{F8H7OH} = 0.05$, there were few differences in the domain shapes as determined from the images of the DPPC monolayer. Strictly speaking, the size of the ordered domains and their ratio per frame increase slightly. As seen from the images of the monolayers corresponding to $X_{F8H7OH} = 0.1$ and 0.2, the addition of *F*8*H*7OH makes the ordered domain round in shape, similar to what was seen in the corresponding BAM images (Fig. 4). The ordered domains corresponding to $X_{F8H7OH} = 0.2$ are smaller in size. Moreover, it is worth noting that the domain goes from being round in shape to being rough edged with an increase in the surface pressure from 15 to 20 mN m^{-1} (the forth column). With a further increase in compression, the ordered domains fuse with each other, and the contrast of the image becomes unclear (25 mN m^{-1}). A similar behavior is observed in the case of the DPPC/*F*4*H*11OH system[19]. However, in that system, the edges of the ordered domains become much more indistinguishable as the surface pressure increases. That is, the ordered domains dissolve into the disordered regions with the increase in the surface pressure. In the present case, the lack of clarity of the images is considered to arise from the undesirable interaction between the FM probe and the *F*8*H*7OH molecules. However, if that were the case, this phenomenon of lack of clarity should have been observed in the corresponding BAM images as well. Nevertheless, these variations in the domain shape support the observation that the two components exhibit miscibility because the composition at the edges of the ordered domains is different from that of the DPPC monolayers, and as a result, the appearance of the ordered domains varies with X_{F8H7OH}. For $X_{F8H7OH} \geq 0.3$, the FM images remain optically homogeneous in contrast, regardless of the surface pressure. This result is in good agreement with the results obtained using BAM and implies that, for X_{F8H7OH} values greater than 0.3, the coexistence state of the disordered and ordered domains may be visually discernible at the nanometer scale (see the next section). Figure 6 shows plots of the percentage of the ordered domain per frame of the FM images (Fig. 5) as a function of the surface pres-

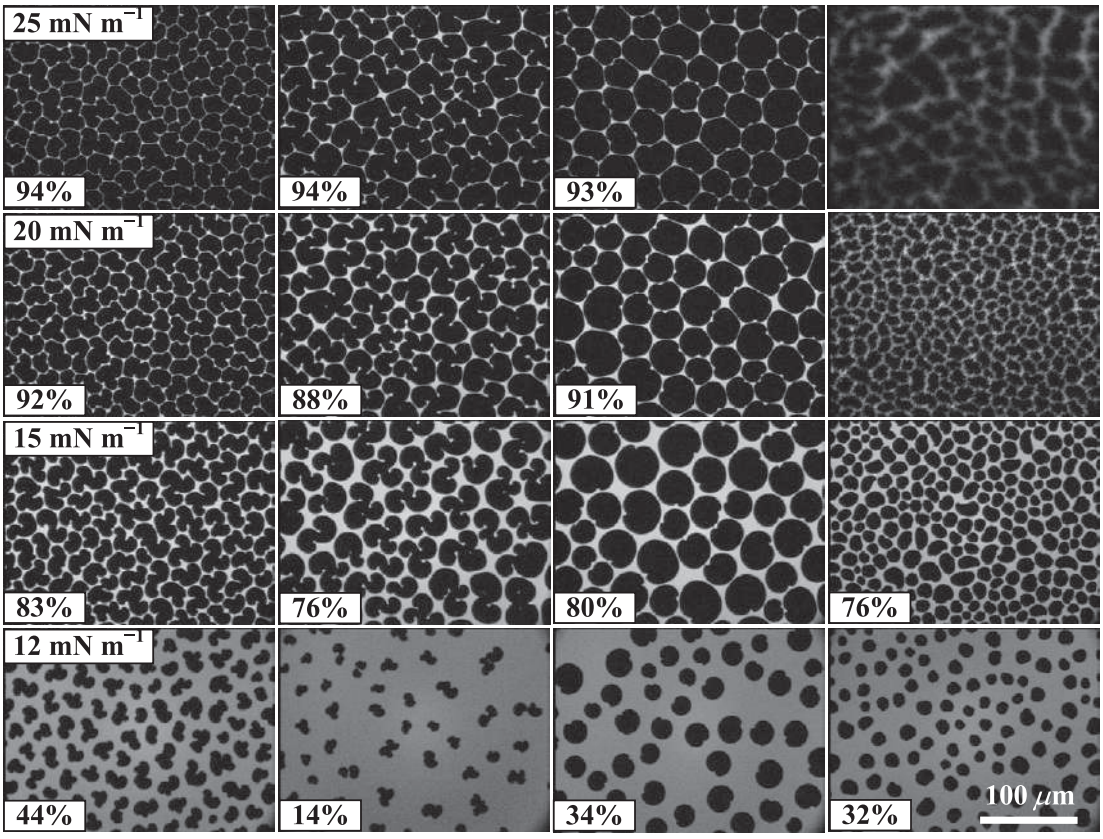

Fig. 5 FM images of the binary DPPC/*F*8*H*7OH monolayers for X_{F8H7OH} = 0 (DPPC), 0.05, 0.1, and 0.2 at 12, 15, 20, and 25 mN m^{-1} on 0.15 M NaCl at 298.2 K. The monolayers contain 1 mol% of fluorescent probe (NBD-PC). The percentage (%) in lower-left corner exhibits the ratio of ordered domains (dark contrast) per micrograph. The scale bar in the lower right represents 100 μm.

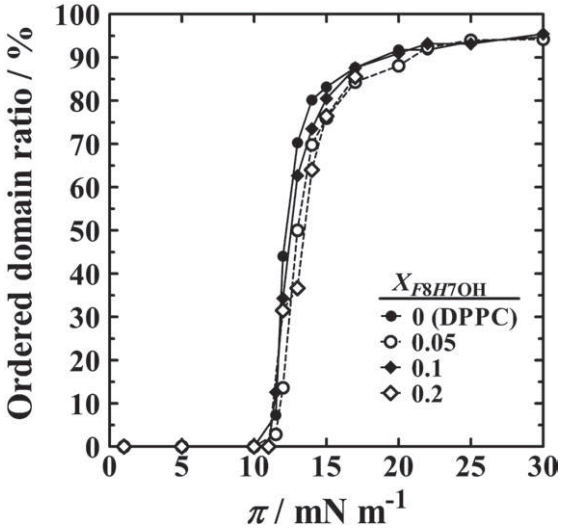

Fig. 6 Surface-pressure dependence of the ratio of ordered domain area (dark contrast) in FM images of the binary DPPC/*F*8*H*7OH monolayers for X_{F8H7OH} = 0, 0.05, 0.1, and 0.2.

sure. The ordered domain ratio for the compositions shown increases monotonically with an increase in the surface pressure, eventually reaching ~95% at 30 mN m^{-1}. Therefore, this result suggests that the addition of *F*8*H*7OH in small amounts does not induce the fluidization of DPPC monolayers.

3.6 AFM observations

The phase behavior for $0.3 < X_{F8H7OH} < 1$ could not be characterized using either BAM or FM because of the limited optical resolution and magnification of the microscopes employed. Therefore, the morphologies of the corresponding single-layer Langmuir-Blodgett (LB) films, which were transferred onto a mica substrate, had to be imaged using AFM. Films formed by the LB technique are subject to the possibility that their original monolayer structures may be changed by the electric charge present on the samples as well as by other physical factors during the deposition process. AFM images may, therefore, not provide completely accurate information regarding the phase behavior at the air–water interface. The AFM topo-

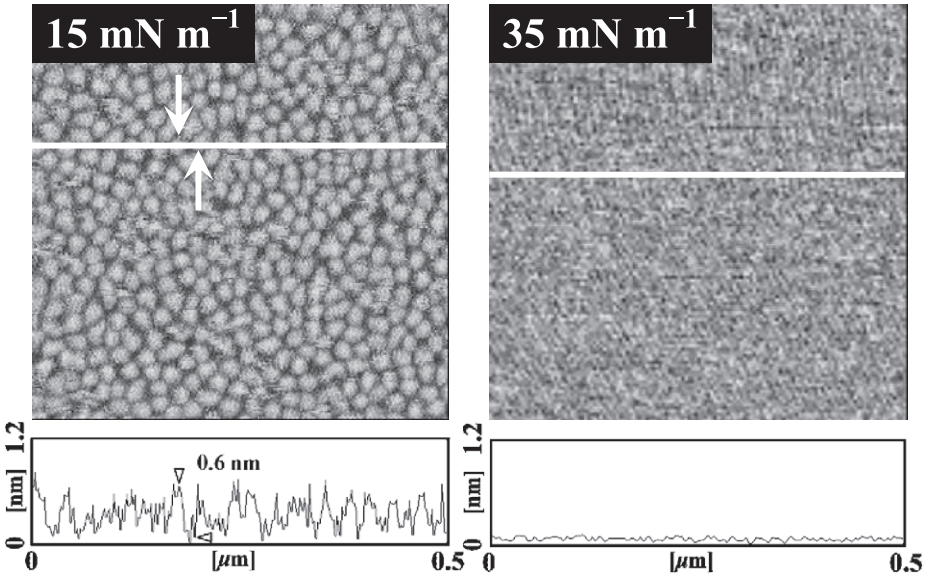

Fig. 7 Typical AFM topographic images of single *F*8*H*7OH monolayers at 15 and 35 mN m^{-1}. The scan area is 500 × 500 nm. The cross-sectional profiles along the scanning line (white line) are given just below the respective AFM images. The height difference between the arrows is indicated in the cross-sectional profile.

graphical images of pure DPPC monolayers at 35 mN m^{-1} were optically homogeneous (data not shown). The AFM images of the individual *F*8*H*7OH monolayers at 15 and 35 mN m^{-1} are shown in Fig. 7. At 15 mN m^{-1}, *F*8*H*7OH organizes into monodispersed 2D surface micelles having a characteristic diameter of 19.4 ± 2.0 nm and height of 0.6 ± 0.1 nm. Each surface micelle was estimated to be composed of ~900 molecules. Further compression, that is, an increase in the surface pressure to 35 mN m^{-1}, causes the surface micelles to coalesce; however, there is no discernible change in their morphology[3]. It is considered that these micelles are formed owing to a weak van der Waals interaction between the fluorocarbon molecules. Thus, lateral compression decreases the intermolecular distance, causing the micelles to disappear. However, in some cases, the micelles continue to appear even at high surface pressures[5]. LB films of partially fluorinated compounds often exhibit topologies that consist of surface micelles; these compounds include partially fluorinated alkanoic acids[3, 5] and alkanes[4]. Kato and coworkers have reported that the formation of surface micelles is induced by the rapid evaporation of the solvent when it is being spread on the substrate surface[5].

The AFM images of the two-component system for $X_{F8H7OH} = 0.3$, 0.5, and 0.7, that is, in the cases in which morphological changes could not be observed in the BAM and FM images, are shown in Fig. 8. None of the images indicate the presence of surface micelle assemblies. This is because of the miscibility of the two components or the decrease in *F*8*H*7OH purity or both. The film corresponding to $X_{F8H7OH} = 0.3$ (15 mN m^{-1}) contained a number fragments (bright contrast) composed almost completely of DPPC. The height difference between these fragments and the surrounding network (dark contrast) of *F*8*H*7OH was ~ 0.8 nm. Further compression, that is, an increase in the surface pressure to 35 mN m^{-1}, caused these fragments to disperse. This means that the fragmentation of DPPC monolayers is induced by the surface pressure. That is, the relatively weak van der Waals interaction or cohesive force between the perfluorooctyl moieties contributes to the dispersion of the fragments owing to the decrease in the distance between the DPPC and *F*8*H*7OH molecules upon lateral compression. In the case of the film corresponding to $X_{F8H7OH} = 0.5$, the fragments, which had a height difference of ~0.3 nm, become smaller both in diameter and number. Further, in contrast to the film corresponding to $X_{F8H7OH} = 0.3$, the size and number of the fragments increased with an increase in the surface pressure. In the case of this composition, π-induced fragmentation does not occur; instead, the π-induced growth of the ordered domains is observed commonly. The AFM images of the films corresponding to $X_{F8H7OH} = 0.7$ and 0.9 (data not shown) indicated that the films were quite homogeneous and flat regardless of an increase in surface pressure; this was suggestive of the miscibility of DPPC and *F*8*H*7OH on the nanometer scale.

4 CONCLUSION

The two-component DPPC/*F*8*H*7OH system was systematically characterized at the air-water interface using Langmuir monolayers and LB films of the system. *F*8*H*7OH forms a typical ordered monolayer on 0.15 M NaCl at 298.2

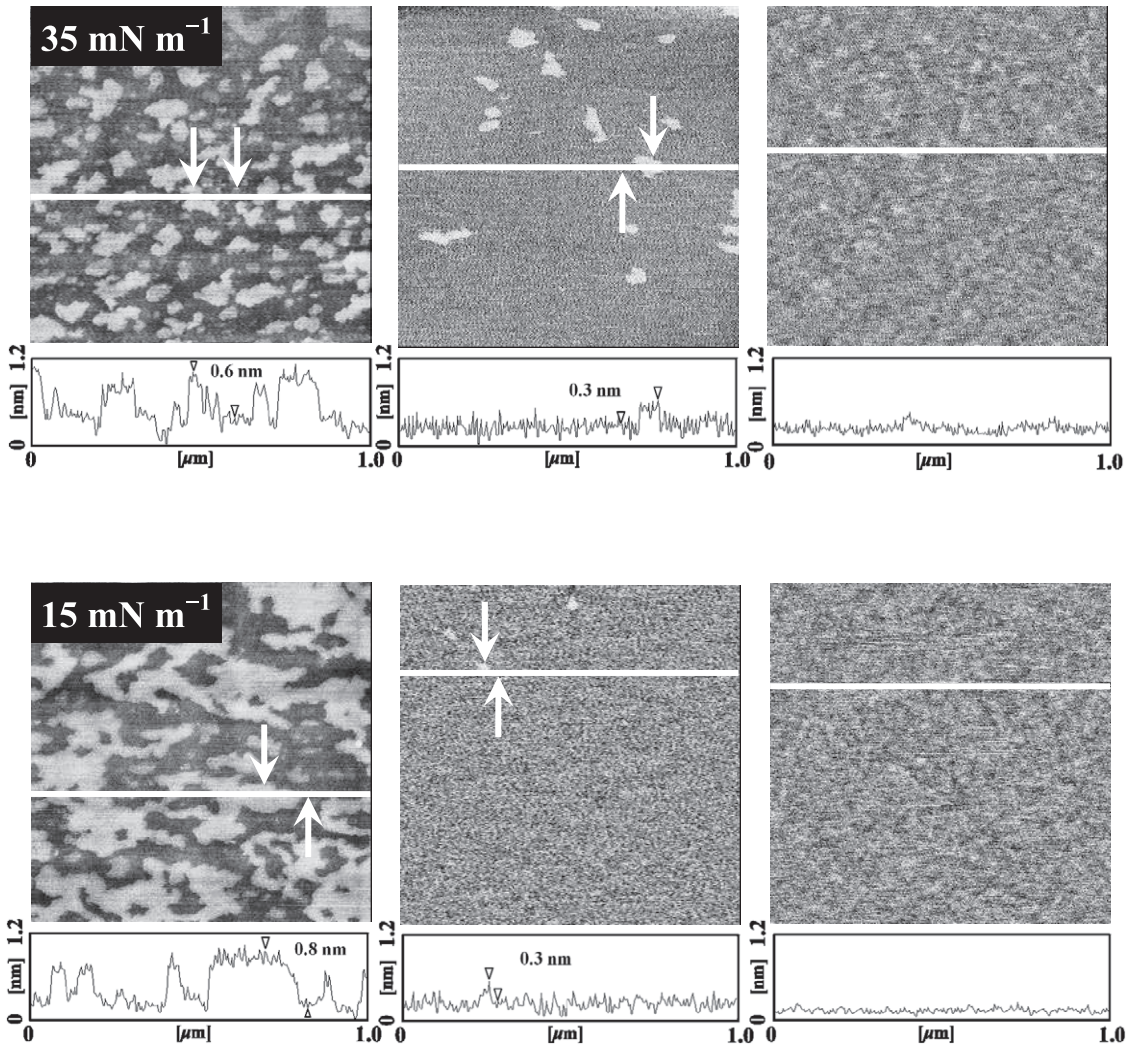

X_{F8H7OH}=0.3 X_{F8H7OH}=0.5 X_{F8H7OH}=0.7

Fig. 8 Typical AFM topographic images of the binary DPPC/*F*8*H*7OH monolayers for X_{F8H7OH} = 0.3, 0.5, and 0.7 at 15 and 35 mN m^{-1}. The scan area is 1 × 1 μm. The cross-sectional profiles along the scanning line (white line) are given just below the respective AFM images. The height difference between the arrows is indicated in the cross-sectional profile.

K. In addition, the AFM images of the monolayer revealed that *F*8*H*7OH organizes into monodispersed 2D surface micelles having a diameter of approximately 20 nm. From a thermodynamic point of view, *F*8*H*7OH was found to be miscible with DPPC in the monolayer state. The excess Gibbs free energy of mixing of the system was calculated on the basis of the additive rule. 2D phase diagrams of the system were also constructed by plotting the surface pressures for the phase transition from disordered to ordered states and of the monolayer collapse with respect to X_{F8H7OH}. On the basis of the diagrams, the binary monolayers were classified into two types: those of the positive azeotropic mixture and those of the negative azeotropic mixture. The interaction parameter and energy were determined while assuming a regular surface mixture. Morphological observations made using BAM and FM supported the observation that the two components exhibited miscibility in the DPPC-rich region on the micrometer scale. Furthermore, miscibility in the *F*8*H*7OH-rich region was confirmed on the nanometer scale using AFM. These results suggest that the interaction modes in the case of DPPC are considerably different and depend on the degree of fluorination of the amphiphile under consideration.

ACKNOWLEDGEMENTS

This work was supported by a Grant-in-Aid for Scientific Research 23510134 from the Japan Society for the Promotion of Science (JSPS). It was also supported by a Grant-in-Aid for Young Scientists (B) 25790020 from JSPS (H.N.).

REFERENCES

1) Riess, J. G. Fluorous micro- and nanophases with a biomedical perspective. *Tetrahedron* **58**, 4113-4131 (2002).
2) Kissa, E., *Fluorinated Surfactants and Repellents. 2nd ed., revised and expanded*. Surfactant Science Series 97; Hubbard, A. T., Ed.; Marcel Dekker Inc.: Basel, New York, pp 1-615 (2001).
3) Ren, Y.; Iimura, K.; Kato, T. Surface micelles of $F(CF_2)_m(CH_2)_{22}COOH$ on the aqueous cadmium acetate solution investigated in situ and ex situ by infrared spectroscopy. *J. Phys. Chem. B* **106**, 1327-1333 (2002).
4) Maaloum, M.; Muller, P.; Krafft, M. P. Lateral and Vertical Nanophase Separation in Langmuir-Blodgett Films of Phospholipids and Semifluorinated Alkanes. *Langmuir* **20**, 2261-2264 (2004).
5) Kato, T.; Kameyama, M.; Ehara, M.; Iimura, K.-i. Monodisperse Two-Dimensional Nanometer Size Clusters of Partially Fluorinated Long-Chain Acids. *Langmuir* **14**, 1786-1798 (1998).
6) Krafft, M. P. Fluorocarbons and fluorinated amphiphiles in drug delivery and biomedical research. *Adv. Drug Deliv. Rev.* **47**, 209-228 (2001).
7) Riess, J. G. Oxygen carriers ("blood substitutes")–raison d'etre, chemistry, and some physiology. *Chem. Rev.* **101**, 2797-2920 (2001).
8) Higgins, C. P.; Luthy, R. G. Sorption of perfluorinated surfactants on sediments. *Environ. Sci. Technol.* **40**, 7251-7256 (2006).
9) Burns, D. C.; Ellis, D. A.; Li, H.; McMurdo, C. J.; Webster, E. Experimental pKa determination for perfluorooctanoic acid (PFOA) and the potential impact of pKa concentration dependence on laboratory-measured partitioning phenomena and environmental modeling. *Environ. Sci. Technol.* **42**, 9283-9288 (2008).
10) Goss, K. U. The pKa values of PFOA and other highly fluorinated carboxylic acids. *Environ. Sci. Technol.* **42**, 456-458 (2008).
11) Riess, J. G. Highly fluorinated amphiphilic molecules and self-assemblies with biomedical potential. *Curr. Opin. Colloid Interf. Sci.* **14**, 294-304 (2009).
12) Riess, J. G. Understanding the fundamentals of perfluorocarbons and perfluorocarbon emulsions relevant to in vivo oxygen delivery. *Artif. Cells Blood Subst. Immobil. Biotechnol.* **33**, 47-63 (2005).
13) Riess, J. G. Perfluorocarbon-based oxygen delivery. *Artif. Cells Blood Subst. Immobil. Biotechnol.* **34**, 567-580 (2006).
14) Veldhuizen, R.; Nag, K.; Orgeig, S.; Possmayer, F. The role of lipids in pulmonary surfactant. *Biochim. Biophys. Acta* **1408**, 90-108 (1998).
15) Krüger, P.; Baatz, J. E.; Dluhy, R. A.; Lösche, M. Effect of hydrophobic surfactant protein SP-C on binary phospholipid monolayers. Molecular machinery at the air/water interface. *Biophys. Chem.* **99**, 209-228 (2002).
16) Yu, S.-H.; Possmayer, F. Lipid compositional analysis of pulmonary surfactant monolayers and monolayer-associated reservoirs. *J. Lipid Res.* **44**, 621-629 (2003).
17) Nakahara, H.; Shibata, O. Langmuir monolayer miscibility of perfluorocarboxylic acids with biomembrane constituents at the air-water interface. *J. Oleo Sci.* **61**, 197-210 (2012).
18) Nakahara, H.; Nakamura, S.; Kawasaki, H.; Shibata, O. Properties of two-component Langmuir monolayer of single chain perfluorinated carboxylic acids with dipalmitoylphosphatidylcholine (DPPC). *Colloids Surf. B* **41**, 285-298 (2005).
19) Nakahara, H.; Ohmine, A.; Kai, S.; Shibata, O. Monolayer compression induces fluidization in binary system of partially fluorinated alcohol (*F4H*11OH) with DPPC. *J. Oleo Sci.*, **62**, 271-281 (2013).
20) Nakahara, H.; Krafft, M. P.; Shibata, A.; Shibata, O. Interaction of a partially fluorinated alcohol (*F8H*11OH) with biomembrane constituents in two-component monolayers. *Soft Matter* **7**, 7325-7333 (2011).
21) Nakamura, S.; Nakahara, H.; Krafft, M. P.; Shibata, O. Two-component Langmuir monolayers of single-chain partially fluorinated amphiphiles with dipalmitoylphosphatidylcholine (DPPC). *Langmuir* **23**, 12634-12644 (2007).
22) Hoda, K.; Nakahara, H.; Nakamura, S.; Nagadome, S.; Sugihara, G.; Yoshino, N.; Shibata, O. Langmuir monolayer properties of the fluorinated-hydrogenated hybrid amphiphiles with dipalmitoylphosphatidylcholine (DPPC). *Colloids Surf. B* **47**, 165-175 (2006).
23) Hiranita, T.; Nakamura, S.; Kawachi, M.; Courrier, H. M.; Vandamme, T. F.; Krafft, M. P.; Shibata, O. Miscibility behavior of dipalmitoylphosphatidylcholine with a single-chain partially fluorinated amphiphile in Langmuir monolayers. *J. Colloid Interf. Sci.* **265**, 83-92 (2003).
24) Nakahara, H.; Lee, S.; Krafft, M. P.; Shibata, O. Fluorocarbon-hybrid pulmonary surfactants for replacement therapy - a Langmuir monolayer study. *Langmuir* **26**, 18256-18265 (2010).
25) Nakahara, H.; Nakamura, S.; Okahashi, Y.; Kitaguchi, D.; Kawabata, N.; Sakamoto, S.; Shibata, O. Examination of fluorination effect on physical properties of saturated long-chain alcohols by DSC and Langmuir

monolayer. *Colloids Surf. B* **102**, 472-478(2013).
26) Nakahara, H.; Lee, S.; Sugihara, G.; Shibata, O. Mode of interaction of hydrophobic amphiphilic α-helical peptide/dipalmitoylphosphatidylcholine with phosphatidylglycerol or palmitic acid at the air-water interface. *Langmuir* **22**, 5792-5803(2006).
27) Nakahara, H.; Tsuji, M.; Sato, Y.; Krafft, M. P.; Shibata, O. Langmuir monolayer miscibility of single-chain partially fluorinated amphiphiles with tetradecanoic acid. *J. Colloid Interf. Sci.* **337**, 201-210(2009).
28) Nakahara, H.; Shibata, O.; Moroi, Y. Examination of surface adsorption of sodium chloride and sodium dodecyl sulfate by surface potential measurement at the air/solution interface. *Langmuir* **21**, 9020-9022 (2005).
29) Nakahara, H.; Shibata, O.; Rusdi, M.; Moroi, Y. Examination of Surface Adsorption of Soluble Surfactants by Surface Potential Measurement at the Air/Solution Interface. *J. Phys. Chem. C* **112**, 6398-6403(2008).
30) Matsumoto, Y.; Nakahara, H.; Moroi, Y.; Shibata, O. Langmuir monolayer properties of perfluorinated double long-chain salts with divalent counterions of separate electric charge at the air-water interface. *Langmuir* **23**, 9629-9640(2007).
31) *CRC Handbook of Chemistry and Physics*. 91st ed.; Haynes, W. M., Ed.; CRC Press: Boca Raton, London, pp2610., pp 2610(2010).
32) Nakahara, H.; Lee, S.; Shibata, O. Pulmonary surfactant model systems catch the specific interaction of an amphiphilic peptide with anionic phospholipid. *Biophys. J.* **96**, 1415-1429(2009).
33) Goodrich, F. C. In *Proceeding of 2nd International Congress on Surface Activity, J. H. Schulman ed.*, London, 1957; Butterworth & Co.: London, 1957; p 85.
34) Marsden, J.; Schulman, J. H. *Trans. Faraday Soc.* **34**, 748-758(1938).
35) Shah, D. O.; Schulman, J. H. *J. Lipid Res.* **8**, 215-226 (1967).
36) Joos, P.; Demel, R. A. The interaction energies of cholesterol and lecithin in spread mixed monolayers at the air-water interface. *Biochim. Biophys. Acta* **183**, 447-457(1969).
37) Savva, M.; Acheampong, S. The interaction energies of cholesterol and 1,2-dioleoyl-sn-glycero-3-phosphoethanolamine in spread mixed monolayers at the air-water interface. *J. Phys. Chem. B* **113**, 9811-9820 (2009).
38) Thirumoorthy, K.; Nandi, N.; Vollhardt, D. Role of dipolar interaction in the mesoscopic domains of phospholipid monolayers: dipalmitoylphosphatidylcholine and dipalmitoylphosphatidylethanolamine. *Langmuir* **23**, 6991-6996(2007).
39) Leiske, D. L.; Meckes, B.; Miller, C. E.; Wu, C.; Walker, T. W.; Lin, B.; Meron, M.; Ketelson, H. A.; Toney, M. F.; Fuller, G. G. Insertion mechanism of a poly(ethylene oxide)-poly(butylene oxide)block copolymer into a DPPC monolayer. *Langmuir* **27**, 11444-11450(2011).
40) Scholtysek, P.; Li, Z.; Kressler, J.; Blume, A. Interactions of DPPC with semitelechelic poly(glycerol methacrylate)s with perfluoroalkyl end groups. *Langmuir* **28**, 15651-15662(2012).